Nuclear Engineering and Design 238 (2008) 2828–2833

Contents lists available at ScienceDirect

Nuclear Engineering and Design

journal homepage: www.elsevier.com/locate/nucengdes

Auto MOC—A 2D neutron transport code for arbitrary geometry based on the method of characteristics and customization of AutoCAD

Qichang Chen, Hongchun Wu, Liangzhi Cao*

School of Nuclear Science and Technology, Xi'an Jiaotong University, Xi'an Shaanxi 710049, China

ARTICLE INFO

Article history:
Received 17 December 2007
Received in revised form 23 April 2008
Accepted 23 April 2008

ABSTRACT

A new 2D neutron transport code AutoMOC for arbitrary geometry has been developed. This code is based on the method of characteristics (MOCs) and the customization of AutoCAD. The MOC solves the neutron transport equation along characteristic lines. It is independent of the geometric shape of boundaries and regions. So theoretically, this method can be used to solve the neutron transport equation in highly complex geometries. However, it is important to describe the geometry and calculate intersection points of each characteristic line with every boundary and region in advance. In complex geometries, due to the complications of treating the arbitrary domain, the selection of geometric shapes and efficiency of ray tracing are generally limited. The geometry treatment through the customization of AutoCAD, a widely used computer-aided design software package, is given in this paper. Thanks to the powerful capability of AutoCAD, the description of arbitrary geometry becomes quite convenient. Moreover, with the language Visual Basic for Applications (VBAs), AutoCAD can be customized to carry out the ray tracing procedure with a high flexibility in geometry. The numerical results show that AutoMOC can solve 2D neutron transport problems in a complex geometry accurately and effectively.

1. Introduction

In the design of advanced nuclear reactors, solving the neutron transport equation in complex geometry will be required. However, most of the existing deterministic neutron transport codes are geometry-dependent and difficult to extend to arbitrary geometry. The method of characteristics (MOCs) solves the neutron transport equation along each characteristic line. Theoretically it is independent of the geometric shape of boundary and region. But it is important to describe the geometry and calculate intersection points of each characteristic line with every boundary and region in advance. In most of the computational algorithms (Askew, 1972; Cho and Hong, 1996; Hong and Cho, 1998; Goldberg et al., 1995; Halsall, 1996; Wu and Roy, 2003) based on the MOC, the description of arbitrary geometry still presents difficulties and the ray tracing procedure is geometry-dependent. Thus in complex geometry, due to the great difficulty of treating the arbitrary domain, the selection of geometry shape and the efficiency of ray tracing are generally limited.

Recently, some new MOC codes (Sugimura et al., 2007; Jevremovic et al., 2001, 2002) based on the *R*-function solid modelers, such as ANEMONA (Jevremovic et al., 2001, 2002) have been developed. This solid modeler has high flexibility and the power of the combinatorial geometry method (Postma and Vujic, 1999). Thus the treatment of arbitrary domain for complex geometry is possible. However, the types of outer boundary shapes and background meshes are still limited to the types provided in the code, and in the case of reflective boundary condition, the number of azimuthal angles must be consistent with the selected outer boundary shapes.

To make the geometry description more efficient and convenient, and remove these limitations on using MOC in more complex geometry, a more powerful geometry treatment method, the customization of AutoCAD, is introduced in this paper. As a well-known computer-aided design software package, AutoCAD has a powerful capability for graphics. Any type of geometric shape can be easily described in AutoCAD. The user can draw arbitrary geometry using the basic primitives such as line, arc and spline, or with typical primitives such as regular polygon, non-regular polygon, circle, ellipse or a combination of them. In the description of the geometry, the selection of the outer boundary or region shape is very flexible; the geometry can be quite arbitrary and can be rotated through an angle of any degree. In the ray tracing procedure, the language Visual Basic for Applications (VBAs) can be used to customize AutoCAD. The customized macro can be executed in AutoCAD, and ray tracing will be carried out uniformly regardless of the geometric shape. In addition, the directional interpolation method for the

* Corresponding author. Tel.: +86 29 82663285; fax: +86 29 82667802.
E-mail address: caolz@mail.xjtu.edu.cn (L. Cao).

0029-5493/$ – see front matter © 2008 Elsevier B.V. All rights reserved.
doi:10.1016/j.nucengdes.2008.04.014

reflective boundary condition is introduced in this paper, so the number of azimuthal angles can be selected according to the user's requirements.

The paper is organized as follows. In Section 2, the introduction of the MOC and the directional interpolation method for the reflective boundary condition is introduced briefly. In Section 3, the geometry pretreatment based on the customization of AutoCAD is discussed. In Section 4, the numerical results for several test problems are given. Finally, some conclusions are summarized in Section 5.

2. Model of MOC

2.1. Equations of the MOC

In the MOC, the neutron transport equation is solved along characteristic lines in selected directions (Kugo, 2002). The azimuthal angles are selected uniformly. For polar angles, two optimal polar angles and their corresponding weights (Leonard and McDaniel, 1995) or a standard Gauss-Legendre quadrature set can be used. The space domain is subdivided into many background meshes or regions. In each mesh or region, the source distribution is usually assumed to be constant. Taking the one-group transport equation as an example, the balance equation along a characteristic line can be written as

$$\frac{\mathrm{d}}{\mathrm{d}s}\psi_{i,k}(s,\Omega_m)+\Sigma_{t,i}\psi_{i,k}(s,\Omega_m)=Q_i(\Omega_m) \tag{1}$$

where s is the distance along the characteristic line; $\Sigma_{t,i}$ is the total cross-section of the region i; $\psi_{i,k}(s,\Omega_m)$ is the angular flux in the region i at distance s along the line segment k; $Q_i(\Omega_m)$ is the average source in the region i.

Eq. (1) can be solved analytically:

$$\psi_{i,k}(s,\Omega_m)=\psi_{i,k}^{\mathrm{in}}(\Omega_m)\exp(-\Sigma_{t,i}s)+\frac{Q_i(\Omega_m)}{\Sigma_{t,i}}(1-\exp(-\Sigma_{t,i}s)) \tag{2}$$

where $\psi_{i,k}^{\mathrm{in}}(\Omega_m)$ is the angular flux at the starting point where a neutron enters into the region i along segment k.

According to Eq. (2) the outgoing neutron angular flux from region i along segment k with the length of this segment $s_{i,k}$ is written as

$$\psi_{i,k}^{\mathrm{out}}(\Omega_m)=\psi_{i,k}^{\mathrm{in}}(\Omega_m)\exp(-\Sigma_{t,i}s_{i,k})+\frac{Q_i(\Omega_m)}{\Sigma_{t,i}}(1-\exp(-\Sigma_{t,i}s_{i,k})) \tag{3}$$

By integrating the angular flux along the segment k, the segment average angular flux is obtained as

$$\bar{\psi}_{i,k}(\Omega_m)=\frac{Q_i(\Omega_m)}{\Sigma_{t,i}}+\frac{\psi_{i,k}^{\mathrm{in}}(\Omega_m)-\psi_{i,k}^{\mathrm{out}}(\Omega_m)}{\Sigma_{t,i}s_{i,k}} \tag{4}$$

Similarly, the region average angular flux can be obtained

$$\bar{\psi}_i(\Omega_m)=\frac{\sum_k\bar{\psi}_{i,k}(\Omega_m)s_{i,k}\delta A_k}{\sum_k s_{i,k}\delta A_k} \tag{5}$$

where δA_k is the width of the segment k.

The region average scalar flux can be obtained as

$$\phi_i=\sum_{m=1}^{M}\omega_m\bar{\psi}_i(\Omega_m) \tag{6}$$

where ω_m is the weight for direction Ω_m, M is the total number of directions.

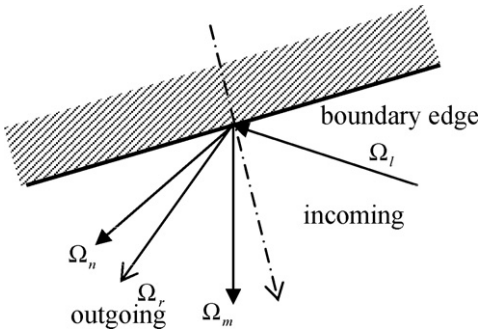

Fig. 1. Interpolation of reflective boundary condition.

2.2. Treatment of reflective boundary condition

In most of the existing MOC codes, the treatment of reflective boundary condition have some limitations based on the shape of the outer boundary.

Here the directional interpolation method is proposed for use in the treatment of a reflective boundary condition. With this method, not only do the rays not need to return exactly to the starting point (Roy, 1998), but also the number of azimuthal angles can be selected freely regardless of the outer boundary shape. As in ANEMONA (Jevremovic et al., 2001), the boundary is subdivided into edges by the regions enclosed by this boundary, and it is assumed that the incoming angular fluxes for every ray is the average of outgoing angular flux on the same boundary edge.

For the reflective direction the directional interpolation method is used, as shown in Fig. 1. The incoming flux will be interpolated by the adjacent outgoing fluxes in the ray directions; and the interpolation coefficients will be calculated according to the location of the outgoing direction in the angle zone, as expressed by Eqs. (7) and (8):

$$\psi_l=\psi_{\mathrm{r}}=C_l\psi_m+(1-C_l)\psi_n \tag{7}$$

and

$$C_l=\frac{\theta_n-\theta_{\mathrm{r}}}{\theta_n-\theta_m} \tag{8}$$

where ψ_l is the incoming angular flux from the outer boundary in direction l; ψ_r is the reflective outgoing angular flux; ψ_m, ψ_n are the adjacent outgoing fluxes; C_l is the interpolation coefficient of direction l; θ_r is the angle of the reflective outgoing direction; θ_m, θ_n are the angles of the adjacent outgoing direction.

3. Geometry pretreatment based on the customization of AutoCAD

3.1. Geometry description

To solve the neutron transport equation in a certain geometry by AutoMOC, the user first draws graphs in AutoCAD, as shown in Fig. 2. Thanks to the powerful capability in graphics, the geometry description in AutoCAD is quite convenient. The user can draw graphs by typical primitives such as regular polygon, non-regular polygon, rectangular, circle and ellipse or the combination thereof. Of course the user can also use lines, arcs and spline curves to describe arbitrary domains. Moreover, AutoCAD provide a great many commands for the modification of graphs such as "array", "offset", "rotate", "trim", etc. So it is quite efficient and convenient to describe any type of geometry with AutoCAD.

The area each region can be calculated automatically. And the outer boundary can be selected and specified. It can be composed of

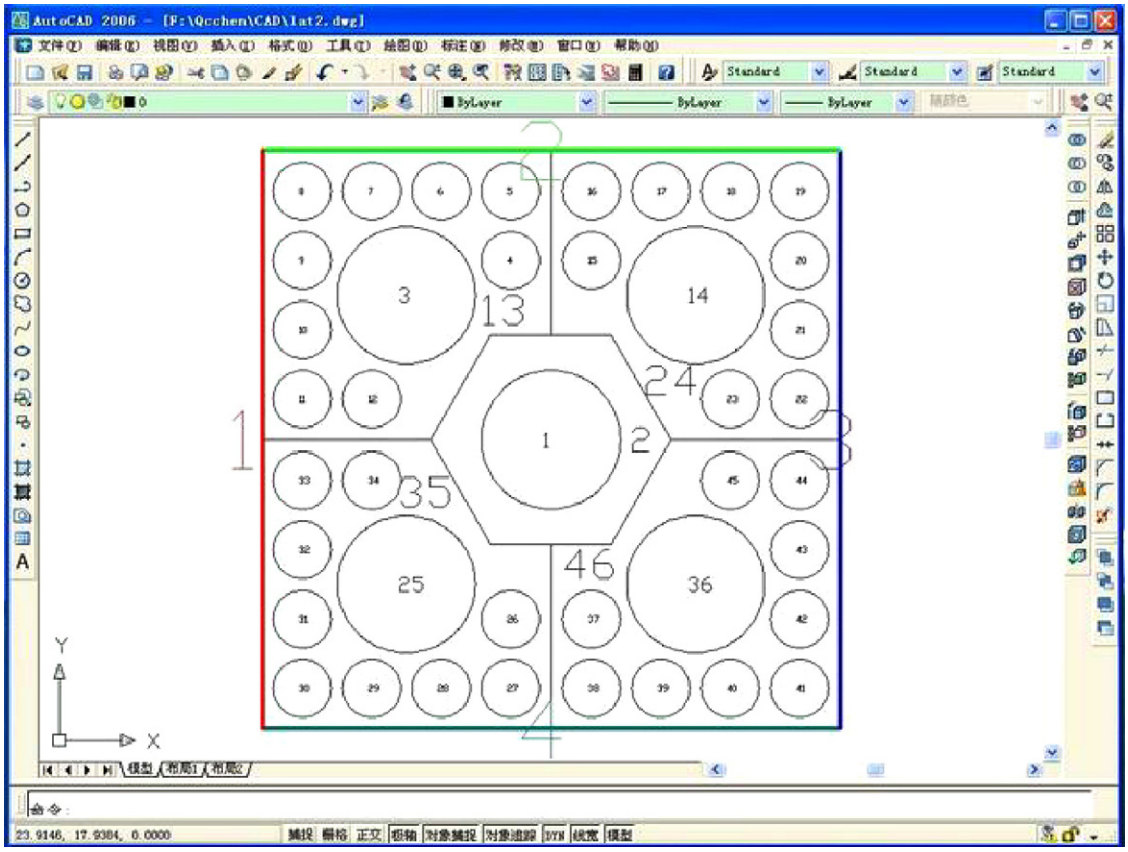

Fig. 2. Geometry description in the AutoCAD.

several boundary segments that can be lines, arcs, splines, ellipses, etc. The regions and boundaries can be numbered automatically by the customized macro. In order to treat the boundary condition, the user also has to specify the regions enclosed by each segment of boundary, and then the boundary segments will be subdivided into edges for the treatment of the boundary conditions.

3.2. Ray tracing

The ray tracing procedure is carried out by a macro that is customized with the VBA language. Before the ray tracing, the outer boundary will be checked to ensure the boundary is closed. The density of characteristic lines and the number of azimuthal angles should be specified by the user. Due to the directional interpolation method, the number of azimuthal angles can be selected without regard to the outer boundary shape. Then characteristic lines will be generated automatically according to the width and the azimuthal angles specified by the user as shown in Fig. 3. And all intersection points of each characteristic line with every boundary and region are obtained. It should be noted that the ray tracing in AutoMOC is applied for the whole geometry, and the region shape can be irregular.

All characteristic line information, including the start point, end point, region/boundary number passed through, segment length in every region, etc., is written into a tracking file. This tracking file is an input file of the MOC code.

4. Numerical validation

A new MOC code named AutoMOC, with geometry treatment based on the customization of AutoCAD, has been developed. The numerical results for several test problems are given here.

4.1. ISSA problem

The first test case is the ISSA 1D problem (Issa et al., 1986) as show in Fig. 4. Reflective boundary condition and vacuum boundary condition are applied in the left and right side, respectively.

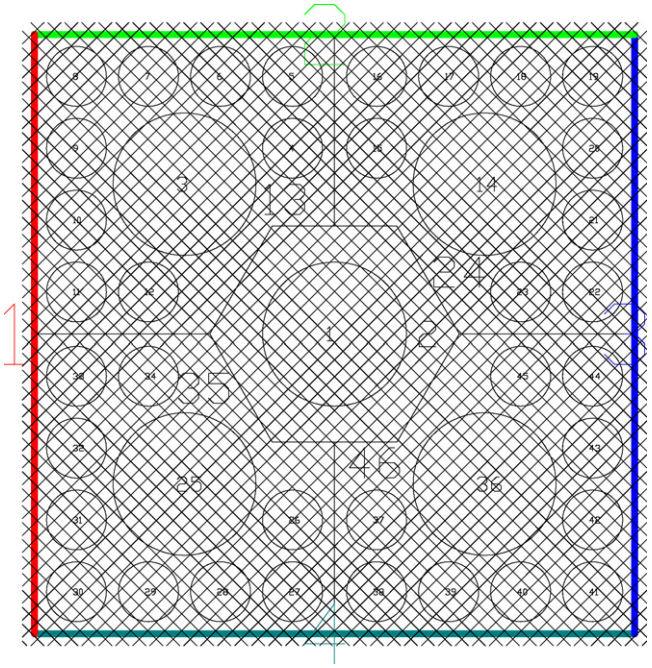

Fig. 3. Ray traces in the AutoMOC.

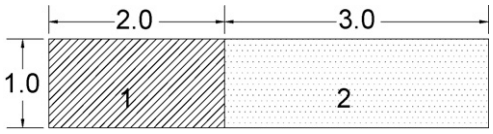

Fig. 4. ISSA 1D problem geometry (cm^{-1}).

Table 1
Macroscopic cross-sections of ISSA problem

Cross-Section	Σ_t (cm^{-1})	$\nu\Sigma_f$ (cm^{-1})	Σ_s (cm^{-1})
Region 1	1.0	1.0	0.5
Region 2	0.8	0.0	0.4

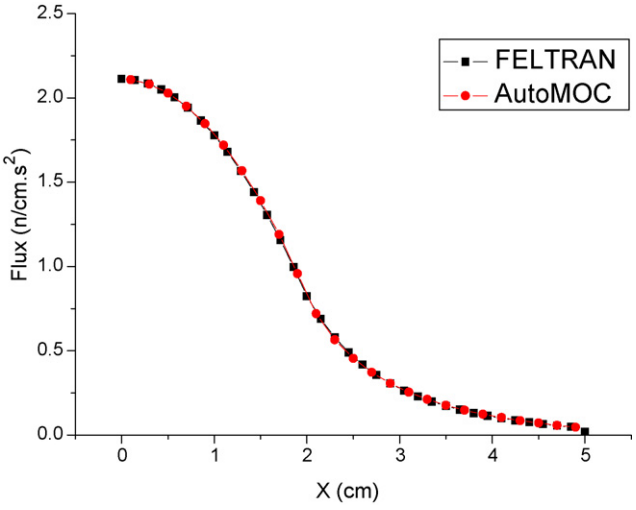

Fig. 5. Neutron flux distribution of ISSA problem.

Table 2
Comparison of *k*-effective of ISSA problem

Code	*k*-effective				
AutoMOC	2* 1.64479	4* 1.67599	6* 1.67738	8* 1.67884	16* 1.67881
ANISN	S_2 –	S_4 –	S_6 1.6772	S_8 –	S_{16} 1.6784
FELTRAN	P_1 1.6451	P_3 1.6751	P_5 1.6771	– –	– –
MCNP	1.67876 ± 0.00036				

* Number of azimuthal angles for AutoMOC.

Here it is extended to a 2D problem by using a reflective boundary condition in the *y*-direction. The macroscopic cross-sections of each material are given in Table 1. The calculated results from AutoMOC are compared with FELTRAN (Feyzi, 1996), ANISN and MCNP. Table 2 shows the comparisons of *k*-effective with different number of directions. Two optimal polar angles (0–π/2) (Leonard and McDaniel, 1995) were used in AutoMOC. The neutron flux distribution is shown in Fig. 5. One can see that both *k*-effective and flux distribution are in good agreement with the reference results. The difference in *k*-effective between AutoMOC and MCNP was 0.003% when 16 azimuthal angles were adopted. In the MCNP calculation, 20,000 histories with 500 cycles including 50 inactive cycles were run.

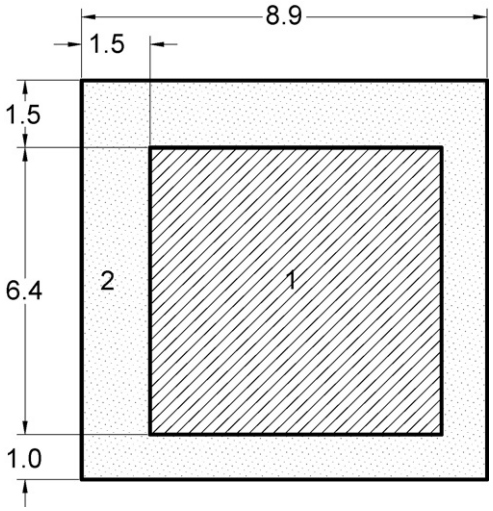

Fig. 6. BWR problem geometry (cm^{-1}).

Table 4
Comparison of *k*-infinite and neutron flux distribution of BWR problem

Flux	Group 1		Group 2		*k*-Infinite
	Region 1	Region2	Region 1	Region2	
AutoMOC	1.0	0.9278	0.3530	0.4512	1.2137
SURCU	1.0	0.9271	0.3529	0.4509	1.2127
Difference (%)	–	0.075	0.028	−0.066	0.082

4.2. BWR problem

This problem is a homogeneous BWR cell (Stepanek et al., 1983a,b). The central homogenized fuel region is surrounded by water moderator as presented in Fig. 6. The macroscopic cross-sections for each region are given in Table 3. The reference solution is given by SURCU (Stepanek et al., 1983a,b), a code based on integral transport method. Table 4 shows the comparison of *k*-infinite and neutron flux distribution. Eight uniform azimuthal angles (0–π) and two optimal polar angles (0–π/2) were used. The results show good agreement in *k*-infinite and flux distribution between AutoMOC and SURCU. The difference in *k*-infinite was 0.082% and the maximal difference in region flux was 0.075%.

4.3. Irregular 2D geometry problem

To test the flexibility of AutoMOC for complex geometry, a one-group problem with irregular geometry is designed here as shown

Table 3
Macroscopic cross-sections of BWR problem

Energy group	Material	$(\nu\Sigma_f)_g$ (cm^{-1})	$\Sigma_{g\to1}$ (cm^{-1})	$\Sigma_{g\to2}$ (cm^{-1})	Σ_t (cm^{-1})	χ_g
1	1	6.203E-3	1.78E-1	1.002E-2	1.96647E-1	1.0
	2	0.0	1.995E-1	2.188E-2	2.22064E-1	
2	1	1.101E-1	1.089E-3	5.255E-1	5.96159E-1	0.0
	2	0.0	1.558E-3	8.783E-1	8.87874E-1	

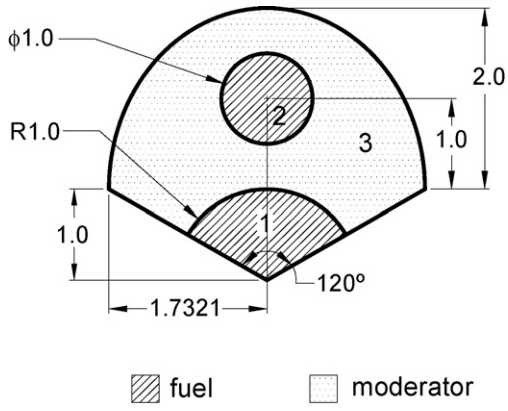

Fig. 7. Irregular geometry problem (cm^{-1}).

Table 5
Cross-sections of Irregular geometry problem

Material	Σ_t (cm^{-1})	$\nu\Sigma_f$ (cm^{-1})	Σ_s (cm^{-1})
Fuel	1.0	1.0	0.7
Moderator	0.8	0.0	0.4

in Fig. 7. It contains two fuel regions and a surrounding moderator region. The cross-sections for the fuel and the moderator are given in Table 5. The outer boundary consists of two line segments with a reflective boundary condition and half an elliptic arc with a vacuum boundary condition. Two different unstructured meshing schemes (500 regions and 1380 regions, respectively) were used as shown in Fig. 8. Eight uniform azimuthal angles (0–π) and four polar angles (0–$\pi/2$) based on Gauss-Legendre quadratures were used. k-Effective and neutron flux for each region are compared with MCNP in Table 6. In the MCNP calculation, 50,000 histories with

Table 6
Comparison of k-effective and flux distribution of irregular geometry problem

		Region 1	Region 2	Region 3	k-Effective
MCNP		0.79818	0.20895	0.15192	1.20173 ± 0.00020
Meshing I	Flux	0.79542	0.21269	0.15288	1.19584
	Difference (%)	−0.346	1.790	0.632	0.490
Meshing II	Flux	0.79769	0.20966	0.15279	1.20162
	Difference (%)	−0.061	0.342	0.567	−0.009

500 cycles including 50 inactive cycles were run. The results show that AutoMOC agrees well with MCNP. The differences in k-effective and maximal region flux decreases with the refined meshes, which in meshing scheme I is 0.490% and 1.790% while in meshing scheme II is −0.009% and 0.567%.

4.4. Multi-cell lattice

To test the calculation speed of AutoMOC relative to Monte Carlo, a multi-cell geometry like a PWR fuel assembly was computed. The geometry of the lattice which has 17×17 pin arrangement is shown in Fig. 9. All the pin cells are uniform fuel cells and are subdivided into five regions. The first two regions correspond to fissile material, the third to cladding material and the last two to moderating material. Six uniform azimuthal angles (0–π) and two optimal polar angles (0–$\pi/2$) were used. The two-group cross-sections are given in Table 7. k-Infinite is compared with MCNP, and the calculation time with different track spacing are presented in Table 8. The MCNP calculations were done with 40,000 neutrons per cycle. After skipping 50 cycles, 250 active cycles were run. One can see that the calculation precision is continuously increasing and the time is almost linearly increasing when the track spacing decreases. The case with 0.04 cm of track spacing can give satisfactory precision with a high computational speed compared with MCNP.

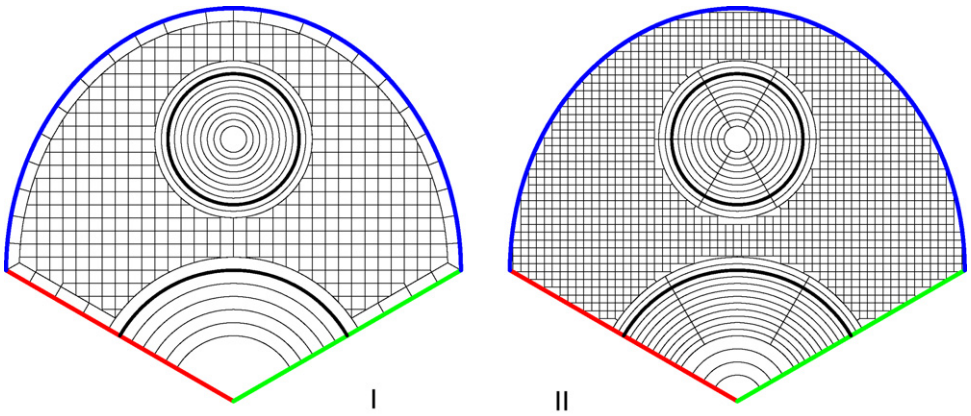

Fig. 8. Unstructured-meshes of irregular geometry problem.

Table 7
Cross-sections of multi-cell lattice

Cross-section	Fuel		Cladding		Moderator	
	Group 1	Group 2	Group 1	Group 2	Group 1	Group 2
Σ_t (cm^{-1})	0.392175	0.622581	0.276383	0.278610	0.439812	1.35565
Σ_a (cm^{-1})	0.029567	0.26285	0.00159	0.004029	0.006534	0.017808
$(\nu\Sigma_f)_g$ (cm^{-1})	0.022141	0.496970	0.0	0.0	0.0	0.0
$(\Sigma_f)_g$ (cm^{-1})	0.00918713	0.206211618	0.0	0.0	0.0	0.0
$\Sigma_{1\to g}$ (cm^{-1})	0.361893	0.000715	0.274505	0.000288	0.411998	0.02128
$\Sigma_{2\to g}$ (cm^{-1})	0.001451	0.358282	0.000774	0.273807	0.002672	1.33517

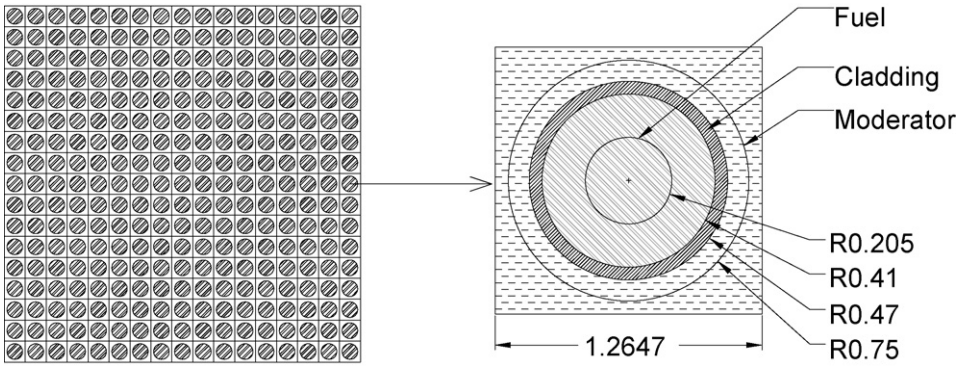

Fig. 9. Multi-cell lattice (cm^{-1}).

Table 8
The *k*-infinite and calculation time comparison of multi-cell lattice

	Track spacing (cm)	Pretreatment time (min)	Calculation time (min)	*k*-Infinite	Difference (%)
AutoMOC	0.08	1.529	0.402	1.065842	0.168
	0.04	2.516	0.772	1.064881	0.078
	0.02	4.807	1.482	1.064520	0.044
	0.01	9.514	2.945	1.064106	0.005
MCNP	–	127.19		1.06405 ± 0.00043	–

In Table 8, it is noticeable that the geometry pretreatment time dominates the total time, but it is needed only once for a series of cases with the same geometry. For example, if it is used to perform a fuel assembly multi-group (typically 69) depletion calculation with many burn-up steps, the time required for geometry pretreatment will be a minor part of that for the whole calculation and the computational efficiency will be higher.

5. Conclusion

A new MOC code AutoMOC, based on the customization of AutoCAD, has been developed. Thanks to the powerful graphics capability of AutoCAD, the description of complex geometry becomes quite efficient and convenient. By using the VBA language to customize AutoCAD, customized ray tracing macro is obtained. The ray tracing procedure can be carried out uniformly regardless of the geometric shape. So the limitations for using MOC in more complex fuel assembly calculations have been removed. In addition, the directional interpolation method for a reflective boundary condition is introduced, so the number of azimuthal angles can be selected freely for any type of outer boundary shape.

Test results show that the AutoMOC can solve the 2D neutron transport problems expediently and automatically in arbitrary geometry. It cannot only give high precision results but it also saves considerable simulation time compared with MCNP. It shows great potential to calculate complex fuel assemblies, especially for multi-group depletion calculation.

Acknowledgements

The authors are very grateful to Ms. Anna Waltar, Dr. Dave Nigg and Dr. Debu Majumdar for their kind revisions of this paper. This work is supported by National Natural Science Foundation of China Grants No. 10475064 and No. 10605017.

References

Askew, R., 1972. A characteristics formulation of the neutron transport equation in complicated geometries. AEEW-M, 1108.
Cho, N.Z., Hong, S.G., 1996. CRX: a transport theory code for cell and assembly calculations based on characteristic method. In: Proceedings of the International Conference on Physics of Reactors, Physor 96, vol. 1, Mito, Ibaraki, Japan, September 16–20, p. A-80.
Feyzi, I., 1996. Verification of the three-dimensional modular nodal method for spherical harmonic equations. Ann. Nucl. Energy 23, 613–616.
Goldberg, L., Vujic, J., Leonard, A., Stackowski, R., 1995. The method of characteristics in general geometry. Trans. Am. Nucl. Soc. 73, 173.
Halsall, M.J., 1996. WIMS7, an overview. In: Proceedings of the International Conference on Physics of Reactors, PHYSOR 96, vol. 1, Mito, Ibaraki, Japan, September 16–20, p. B-1.
Hong, S.G., Cho, N.Z., 1998. CRX: a code for rectangular and hexagonal lattices based on the method of characteristics. Ann. Nucl. Energy 25 (8), 547–565.
Issa, J.G., Riyait, N.S., Goddard, A.J.H., et al., 1986. Multigroup application of the anisotropic FEM code FELTRAN to one, two, three-dimensional and R–Z problems. Prog. Nucl. Energy 18, 251–264.
Jevremovic, T., Ito, T., Inaba, Y., 2002. ANEMONA: multiassembly neutron transport modeling. Ann. Nucl. Energy 29, 2105–2125.
Jevremovic, T., Vujic, J., Tsuda, K., 2001. ANEMONA—a neutron transport code for general geometry reactor assemblies based on the method of characteristics and R-function solid modeler. Ann. Nucl. Energy 28, 125–152.
Kugo, T., 2002. Fast vector computation of the characteristics method. J. Nucl. Sci. Technol. 39, 256–263.
Leonard, A., McDaniel, C.T., 1995. Optimal polar angles and weights. Trans. Am. Nucl. Soc. 73, 171.
Postma, T., Vujic, J., 1999. The method of characteristics in general geometry with anisotropic scattering. Int. Mtg. on Mathematics and Computation, Reactors Physics and Environmental Analysis in Nuclear Applications, M&C, Madrid.
Roy, R., 1998. The cyclic characteristics method. In: Proceedings of the International Topical Meeting on the Physics of Nuclear Science and Technology, vol. 1, Long Island, October 5–8, p. 407.
Stepanek J., Auerbach T., Haelg W., 1983. Calculation of Four Thermal Reactor Benchmark Problems in *X–Y* Geometry, EPRI NP-2855.
Stepanek, J., Auerbach, T., Haelg, W., 1983. Calculation of Four Thermal Reactor Benchmark Problems in *X–Y* Geometry, EPRI NP-2855.
Sugimura, N., Yamamoto, A., Ushio, T., Mori, M., et al., 2007. Neutron transport models of AGEIS: an advanced next-generation neutronics design system. Nucl. Sci. Eng. 155, 276–289.
Wu, G.J., Roy, R., 2003. A new characteristics algorithm for 3D transport calculations. Ann. Nucl. Energy 30, 1–16.